



Synthetic Communications

An International Journal for Rapid Communication of Synthetic Organic Chemistry

ISSN: 0039-7911 (Print) 1532-2432 (Online) Journal homepage: <https://www.tandfonline.com/loi/lsyc20>

N-Mannich bases of benzimidazole as a potent antitubercular and antiprotozoal agents: Their synthesis and computational studies

Vatsal M. Patel, Navin B. Patel, Manuel J. Chan-Bacab & Gildardo Rivera

To cite this article: Vatsal M. Patel, Navin B. Patel, Manuel J. Chan-Bacab & Gildardo Rivera (2020): *N*-Mannich bases of benzimidazole as a potent antitubercular and antiprotozoal agents: Their synthesis and computational studies, Synthetic Communications, DOI: [10.1080/00397911.2020.1725057](https://doi.org/10.1080/00397911.2020.1725057)

To link to this article: <https://doi.org/10.1080/00397911.2020.1725057>



Published online: 14 Feb 2020.



Submit your article to this journal [↗](#)



View related articles [↗](#)



View Crossmark data [↗](#)



N-Mannich bases of benzimidazole as a potent antitubercular and antiprotozoal agents: Their synthesis and computational studies

Vatsal M. Patel^a , Navin B. Patel^b, Manuel J. Chan-Bacab^c, and Gildardo Rivera^d

^aDepartment of Chemistry, Jamanaben Narottambhai Motiram Patel Science College, Surat, India;

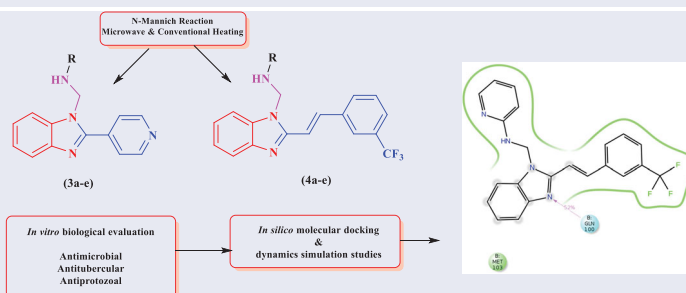
^bDepartment of Chemistry, Veer Narmad South Gujarat University, Surat, India; ^cDepartamento de Microbiología Ambiental y Biotecnología, Universidad Autónoma de Campeche, Campeche, México;

^dLaboratorio de Biotecnología Farmaceutica, Centro de Biotecnología Genómica, Instituto Politécnico Nacional, Reynosa, Mexico

ABSTRACT

This article dealing with the microwave assisted synthesis of *N*-Mannich bases of pyridine clubbed with two different benzimidazole cores with their micromolar biological potency. All the synthesized compounds were evaluated for their *in-vitro* antibacterial, antimycobacterial and antiprotozoal potency. One of the final compound was found to be most active against *M. tuberculosis* (MIC = 3.125 μM) in the primary screening. *N*-Mannich bases of benzimidazole with pyridine-3-amine and 5-methyl-pyridine-2-amine showed potency against *L. mexicana* and *T. cruzi* respectively with IC₅₀ value 0.25 and 1.02 μg/mL. Compound 4a showed good binding energy in the active pocket of receptor (PDB: 4cod) with −11.013 docking score. The stability of docked complex was validated by performing Molecular dynamics (MD) up to 20 ns simulation time. *In silico* ADME parameters and toxicity predicted that the active compounds belong to the Class IV GHS with LD₅₀ value 1360 mg/kg and hence found to be mildly toxic.

GRAPHICAL ABSTRACT



ARTICLE HISTORY

Received 9 December 2019

KEYWORDS

antichagasic; antitubercular; benzimidazole; leishmanicidal; MD simulation; molecular docking

CONTACT Vatsal M. Patel  patelvatsal2119@gmail.com, patelvatsal1904@gmail.com  Department of Chemistry, Jamanaben Narottambhai Motiram Patel Science College, Surat, D C Patel Education Campus, Bharthana, Vesu, Surat, 395017 India; Navin B. Patel  drnavinbpatel@gmail.com  Department of Chemistry, Veer Narmad South Gujarat University, Surat, India.

 Supplemental data for this article can be accessed on the publisher's website

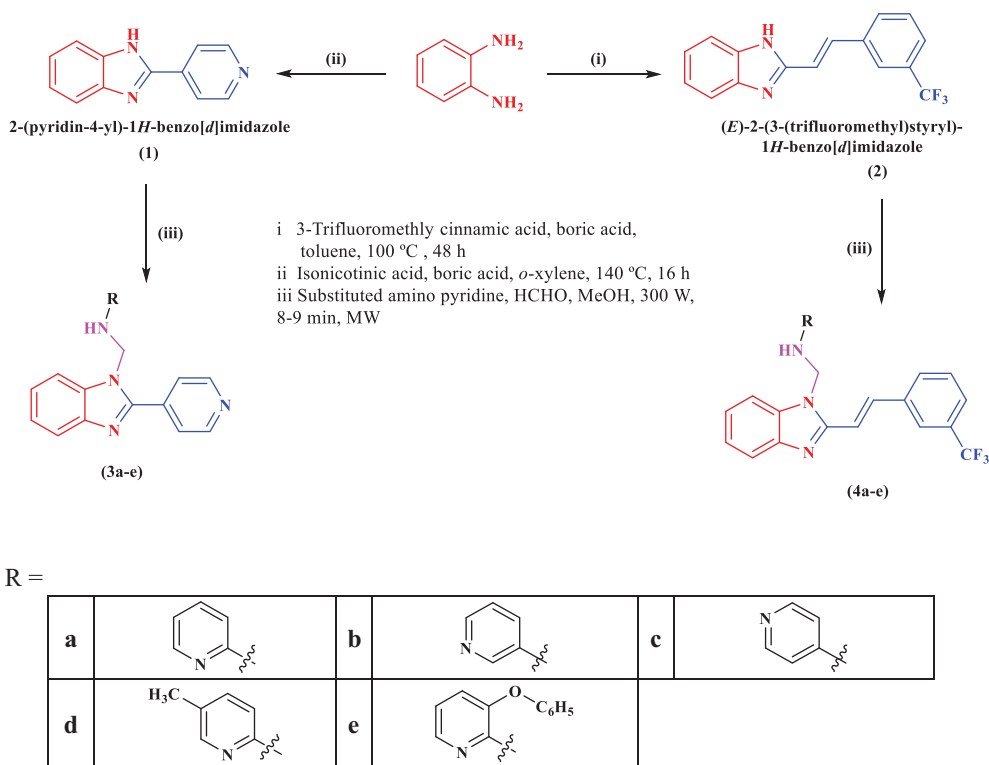
© 2020 Taylor & Francis Group, LLC

Introduction

The parasitic disease leishmaniasis and chagas which are caused by the protozoa *Leishmania mexicana* and protist *Trypanosoma cruzi* are of the most neglected protozoal diseases. The choice for the antiparasitic treatment for this particular class is also limited. The available drugs to treat the particular condition of leishmaniasis are limited to miltefosine, pentavalent antimony, paromomycin, imiquimod, etc. and these pharmaceuticals display low efficacy, serious toxic side effects including patient intolerance, and the induction toward resistant strains opens the door for medicinal chemists to discover of new safe and effective drugs for leishmaniasis treatment.^[1] Anti-chagasic drugs are also confined to particular azole or nitro derivative class viz., benzimidazole or nifurtimox. Researchers around the world continue to search for new efficient compounds in the treatment of this disease. In the continuation of our research^[2] to find the better leishmanicidal and trypanocidal agent, another class of azole is synthesized to get more potent results is described in this article. According to the latest global tuberculosis report-2019 released by the World Health Organization (WHO), tuberculosis (TB) remains the single most lethal infectious disease. As per the report, the cases of extensively drug-resistant (XDR) TB are increased globally by 6 million.^[3] The development for the search of new promising anti-TB agents results in emerging of newer hybrid molecules of class diarylquinolines, oxazolidinones, nitroimidazoles, etc.^[4] Isoniazid (INH) is one of the most effective and widely used drugs for the treatment of TB. InhA, the enoyl-ACP reductase in *Mycobacterium tuberculosis* is found to be an appealing target for the development of novel drugs against TB.^[5] In our previous work, we report the inhibitor that directly targets InhA which resulted in the development of newer series of triazole^[6] and imidazolinone^[7] that are *in-vitro* micromolar inhibitors of *M. tuberculosis* H37Rv.

The biological profile of benzimidazole derivatives occupies an important position in medicinal chemistry.^[8] Benzimidazole has been first synthesized by Hoebrecker in 1872 after that different synthetic routes have been developed to synthesize varied benzimidazole analogous by conventional^[9-11] and non-conventional^[12-15] environmentally benign approach. After the successful evaluation of the very first benzimidazole scaffold in 1944 as an antifungal agent, the numbers of research papers have been published dealing with the various pharmacological importances of benzimidazoles. This versatile heterocyclic core was found to possess bioactivity as analgesic (Bezitramide), antiviral (Enviroxime), antiulcer (Omeprazole, Rabepazole), anti-neoplastic (Nocodazole), antifungal (Ketoconazole, Fluconazole), etc. The presence of benzimidazole nucleus in numerous categories of therapeutic agents^[16] such as antimicrobial,^[17] antivirals,^[18] anti-parasites,^[19] anticancer,^[20] proton pump inhibitors,^[21] immunomodulators,^[22] hormone modulators,^[23] CNS stimulants,^[24] etc. has made it an indispensable anchor for development of new therapeutic agents. On the other hand, Mannich base derivatives of benzimidazole attain great attention in the development of the newer pharmacologically important candidate. Mannich bases of benzimidazole derivative were reported for antimicrobial,^[25] antitubercular,^[26] analgesic and anti-inflammatory activity,^[25] anticancer,^[27] antiviral,^[28] etc.

In view of the preceding facts, we design newer hybrid candidates that combine benzimidazole moiety with pyridine via *N*-Mannich reaction^[29-31] with the aim to produce



Scheme 1. Synthesis of *N*-Mannich base derivatives (3a-e) & (4a-e).

promising antitubercular and antiprotozoal agents. The substitution pattern was carefully chosen to confer different electronic environments to the molecules. All the synthesized molecules were spectrally characterized and subjected to *in-vitro* biological evaluation. Furthermore, all synthesized compounds were *in silico* evaluated for ADME properties, toxicity profile and were docked against an enoyl-acyl carrier protein(ACP)-reductase of *M. tuberculosis* (PDB ID: 4COD)^[32] and ACP reductase of *S. aureus* (PDB ID: 4NZ9).^[33] Molecular dynamics (MD) simulations was performed for up to 20 ns simulation time to investigate ligand-protein complex stability.^[34]

Result and discussion

Chemistry

The synthetic route of the *N*-((2-(pyridin-4-yl)1*H*-benzo[*d*]imidazol-1-yl)methyl)-substituted-aminopyridine (3a-e) and *N*-((2-(3-(trifluoromethyl)styryl)-1*H*-benzo[*d*]imidazol-1-yl)methyl)-substituted-aminopyridine (4a-e) is outlined in Scheme 1. The compound 1 and 2 on reaction with substituted-amino-pyridine and 37% formaldehyde afforded (3a-e) & (4a-e) via microwave induced synthetic approach. The key intermediate 2-(pyridin-4-yl)-1*H*-benzo[*d*]imidazole (1) and 2-(3-(trifluoromethyl)styryl)-1*H*-benzo[*d*]imidazole (2) were obtained by the reaction of *o*-phenylenediamine with isonicotinic acid and 3-trifluoromethyl cinnamic acid respectively. We have carried out the MW synthesis under the Q-proM modified microwave synthesis system. The structures of

Table 1. Antiprotozoal, antibacterial, antifungal and antimycobacterial activity.

Compound No.	Antiprotozoal activity IC ₅₀ µg/mL		Antibacterial activity		Antifungal activity MIC µg/mL	Anti tubercular activity
	<i>L. mexicana</i> MNYC/BZ/ 62/M379	<i>T. cruzi</i> MHOM/MX/ 94/NINOA	<i>E. coli</i> MTCC 442	<i>S. aureus</i> MTCC 96	<i>C. albicans</i> MTCC 227	<i>M. tuberculosis</i> H37Rv
	1	>50	>50	200	250	500
2	>50	>50	200	62.5	500	100
3a	>50	>50	100	250	500	500
3b	2.43	>50	100	100	1000	150
3c	>50	>50	250	500	500	250
3d	0.41	1.02	125	250	500	125
3e	4.59	>50	200	125	500	250
4a	>50	>50	200	25	250	3,125
4b	0.25	1.46	250	62.5	500	62.5
4c	9.60	>50	125	100	1000	150
4d	7.04	>50	62.5	12.5	100	6.25
4e	>50	>50	250	150	1000	125
Miltefosine	0.55	–	–	–	–	–
Benznidazole	–	2.90	–	–	–	–
Ciprofloxacin	–	–	25	50	–	–
Nystatin	–	–	–	–	100	–
Isoniazid	–	–	–	–	–	0.2

compounds were established on the basis of their spectral data. IR spectrum of final compounds showed band at cm^{-1} 3390 for N-H, 3055 for aromatic C-H str., 2868 for methylene C-H str., 1430 for methylene C-H bend., and 1608 for C=N. ¹H NMR spectrum of (**3a–e**) showed singlet at 8.60 for NH which disappeared on D₂O exchange and doublet at 5.02 for CH₂ proton whereas, ¹H NMR (400 MHz, DMSO-*d*₆, δ ppm) spectrum of (**4a–e**) showed signal at 12.69 for NH which disappeared on D₂O exchange, doublet at 7.74 and 7.36 for corresponding styryl CH with coupling constant value 16 Hz confirming the trans isomer and doublet at 5.63 for CH₂ proton. ¹³C NMR (100 MHz, DMSO-*d*₆, δ ppm) spectra of final compounds showed at 61.41 for CH₂, 150.47, 150.05 for C=N, 136.69 to 106.79 for corresponding aromatic carbons and 112.73 for styryl carbon. Moreover, the mass spectrum of these compounds agrees with the molecular weight of the proposed structure. The data generated from all these spectral techniques confirming the formation of a final compounds.

Biology

In-vitro antiprotozoal activity

Compounds **1**, **2**, **3a–e** and **4a–e** were tested *in-vitro* for their potency as antiprotozoal agents against *Leishmania mexicana* and *Trypanosoma cruzi*. Biological assays results on two protozoans parasitic tested are summarized in Table 1. The comparison was made among new benzo[*d*]imidazole derivatives and the antiprotozoal drugs of choice: miltefosine and benznidazole on *L. mexicana* and *T. cruzi*, respectively. From series **3a–e**, compounds **3b**, **3d** and **3e**, showed a biological activity against *L. mexicana*. SAR analysis, showed that a change in the nitrogen atom position drastically affect the biological activity, compounds **3a** and **3c**, have a null leishmanicidal activity (IC₅₀ >50 µg/mL),

however, compound **3b**, showed the higher activity ($IC_{50} = 2.43 \mu\text{g/mL}$). After the incorporation of an electron donating (methyl) group at *para*-position on the pyridine ring enhanced the biological activity, compound **3d** showed a similar IC_{50} value ($0.41 \mu\text{g/mL}$) that miltefosine ($IC_{50} = 0.55 \mu\text{g/mL}$), however a phenoxy group at *ortho*-position on the pyridine ring reduce the effect ten times ($IC_{50} = 4.59 \mu\text{g/mL}$). From series **4a–e**, compounds **4b**, **4c** and **4d** showed also a leishmanicidal activity; in this case, compound **4b** had the best biological effect ($IC_{50} = 0.25 \mu\text{g/mL}$), two times more than miltefosine. SAR analysis showed that the position of the nitrogen atom on the pyridine ring is a key factor in the biological activity. After, substitutions at *para*- and *ortho*-position on the pyridine ring reduce drastically the leishmanicidal effect ($IC_{50} > 50 \mu\text{g/mL}$). A comparison between analogous compounds such as **3a** and **4a** shown that substitution of pyridine ring at 2-position on benzimidazole ring with a 3-trifluoromethylstyryl not affect the biological activity.

The analysis of trypanocidal activity from series **3a–e** shown that *para*-substitution with electron-donating group affects the biological effects drastically, compound **3d** obtained an IC_{50} value ($1.02 \mu\text{g/mL}$) better than benzimidazole ($2.90 \mu\text{g/mL}$). In series **4a–e**, the biological behavior was different; here the position of nitrogen atom in the pyridine ring is the more important factor in the trypanocidal activity. Compound **4b** showed an IC_{50} value of $1.46 \mu\text{g/mL}$, which is better than reference drug.

In-vitro antimicrobial activity

The minimum inhibitory concentrations (MIC) for antimicrobial potency of **1**, **2**, **3a–e** and **4a–e** were screened against two different bacterial strain and one fungal strain. The susceptibility of the organisms was determined by the broth microdilution method and compared with standard drugs; ciprofloxacin and nystatin for antibacterial and antifungal activity respectively. The results of this activity are summarized in Table 1. Initially, compounds **1** and **2** showed moderate to poor activity on both bacterial and fungal strains. Therefore, we had incorporated common amine agents via *N*-Mannich reaction in compounds **1** and **2** to enhance the antimicrobial potency. The results show that there has been no significant improvement for antimicrobial activity while incorporating different pyridine moieties into compound **1**. Interestingly, incorporation of those same pyridine moieties to compound **2** has the positive antimicrobial effect. Firstly we had incorporated simple amino pyridine with different in nitrogen position. **4a** found to possess higher MIC values than control drug. An introduction of electron releasing group ($-\text{CH}_3$) on amino pyridine reagent enhances the antimicrobial potency when it has been incorporated with compound **2**. The compound **4d** exhibited excellent activity ($\text{MIC} = 12.5 \mu\text{M}$) against gram-positive *S. aureus* that compare to control antibacterial drug. Rests of the compounds were poor to moderately active. None of the compounds displayed significant potency against gram-negative *E. coli*. Similar trend has been observed for the minimum fungicidal concentration against *C. albicans*. The incorporation of similar amine component to compound **1** exhibited no interesting results, but with compound **2** some of the derivatives showed relatively significant result as antifungal. Compound **4d** showed potency with MIC value $100 \mu\text{M}$ against *C. albicans*, similar to that of reference drug nystatin. Rests of the compounds showed higher MIC values against the tested fungi species and hence found to be poorly active or non-active.

From SAR studies we may conclude that the presence of styryl functionality and the electron releasing group on amine reagent plays an important role in obtaining better antimicrobial and antifungal activity.

In-vitro antimycobacterial activity

Compounds **1**, **2** and all the newer Mannich derivatives (**3a–e** and **4a–e**) were evaluated to find better antimycobacterial agent against *M. tuberculosis* H37Rv. The evaluation results are given in Table 1. Both the key intermediate **1** and **2** were found to possess higher MIC value and hence found to be poorly active. As discussed previously, five different amine reagents were introduced to both key intermediates to acquire better mycobactericidal candidate. In this studies, we have observed that the change in the position of nitrogen atom in pyridine ring enhance the antimycobacterial potency. Initially three different amino pyridines, viz., 2-amino pyridine, 3-amino pyridine and 4-amino pyridine were selected. Incorporation of these three amine reagents with **1** gives no significant potency. Those amine components while incorporated with **2** enhance the activity. The compound **4d** displayed encouraging potency whereas **4a** found to possess better micromolar potency (MIC = 3.125 μ M) against *M. tuberculosis* compared to control drug. The SAR studies revealed that change in amine component i.e., pyridine-2-amine to pyridine-3-amine decreased the activity by twenty fold. Moreover, introduction of methyl group decreased the activity by two folds. The position of nitrogen atom in pyridine ring and styryl functionality concerned with benzimidazole plays an important role for getting a better antitubercular agent.

Computational studies

In silico molecular docking studies

All the synthesized derivatives **1**, **2**, **3a–e** and **4a–e** were docked against two different targets viz., enoyl-acyl-carrier-protein reductase of *S. aureus* (PDB ID: 4nz9) and enoyl-acyl-carrier-protein reductase of *M. tuberculosis* (PDB ID: 4cod). The results were described in the terms of docking score, XP GScore, glide evdw, glide ecol, glide energy and glide emodel in Tables 2 and 3 respectively. The glide docking score of all the compounds with respect to 4nz9 were in the range from -11.792 to -4.563 , where

Table 2. Docking scores of the compounds **1**, **2**, **3a–e** and **4a–e** with an enoyl-acyl-carrier-protein reductase of *S. aureus* (PDB ID:4nz9).

Compound No.	docking score	XP GScore	glide evdw	glide ecol	glide energy	glide emodel
1	-6.015	-6.021	-25.626	-0.759	-26.385	-37.331
2	-9.87	-9.904	-32.055	-4.722	-36.778	-51.7
3a	-6.299	-6.463	-41.076	-6.236	-47.311	-65.547
3b	-8.617	-8.664	-35.872	-5.167	-41.039	-62.179
3c	-4.563	-4.573	-33.565	-5.416	-38.981	-60.383
3d	-6.146	-6.525	-37.268	-6.39	-43.658	-66.441
3e	-7.776	-7.781	-39.597	-2.913	-42.51	-61.869
4a	-10.528	-10.528	-44.011	-5.869	-49.88	-80.684
4b	-9.692	-9.83	-43.087	2.692	-40.394	-64.128
4c	-8.601	-8.697	-35.511	-5.84	-41.351	-63.435
4d	-11.792	-12.249	-48.446	-5.767	-54.213	-75.542
4e	-7.034	-7.129	-41.051	-1.31	-42.361	-60.071
4nz9_molecule	-10.007	-10.007	-40.801	-7.91	-48.711	-74.439

Table 3. Docking scores of **1**, **2**, **3a–e** and **4a–e** with an enoyl-[acyl-carrier-protein] reductase of *M. tuberculosis* (PDB ID: 4cod).

Compound No.	docking score	XP GScore	glide evdw	glide ecol	glide energy	glide emodel
1	−7.769	−7.775	−27.871	−4.185	−32.056	−42.749
2	−7.664	−7.698	−28.765	−5.450	−34.214	−45.298
3a	−3.331	−4.172	−36.83	−2.48	−39.31	−55.639
3b	−6.288	−6.335	−41.374	−2.119	−43.493	−52.324
3c	−5.139	−5.235	−34.301	−0.594	−34.895	−58.608
3d	−7.626	−7.631	−52.113	−2.464	−54.577	−81.452
3e	−5.416	−5.86	−41.966	−3.246	−45.212	−58.410
4a	−11.013	−11.266	−55.204	−4.873	−60.077	−95.986
4b	−10.154	−11.016	−42.31	−4.402	−46.711	−59.458
4c	−5.352	−6.510	−42.089	−1.427	−43.517	−59.915
4d	−10.679	−10.817	−45.337	−1.119	−46.456	−68.454
4e	−6.168	−7.302	−45.001	−3.086	−48.085	−64.492
4cod_molecule1	−11.160	−11.160	−61.695	−11.75	−73.454	−112.71
4cod_molecule2	−8.523	−8.523	−50.299	−21.305	−71.604	−99.810

compound **4d** showed very good binding energy in the active pocket of receptor with −11.792 docking score (−12.249 XP Gscore), showed most potent as well in wet lab result against *S. aureus* (MIC = 12.5 μ M). It was found to interact with amino acid residues Tyr157 and Tyr147 through π - π stacking and found the potential to inhibit Enoyl ACP reductase of *S. aureus*. **Figure 1a** shows the fit of compound **4d** into the active site of the receptor and the 2D plots of ligand interaction map are shown in **Figure 1b** for the same. The same compound also displayed good binding energy in the active pocket of receptor Enoyl ACP reductase of *M. tuberculosis* with −10.154 docking score, showed moderate potency with *in-vitro* antimycobacterial potency against *M. tuberculosis* with MIC 6.25 μ M. Whereas compound **4a** interacts within the active pocket of the receptor with −11.013 docking score (−11.266 XP Gscore). On the basis of activity data and docking result **4a** and **4d** both had potential to inhibit an Enoyl ACP reductase of *M. tuberculosis*. The binding interactions of both of these compounds are almost similar as both compounds bind with the amino acid residue through hydrogen bonding and π - π stacking with. For compound **4a**, hydrogen bonding and π - π stacking interactions were observed with Ala198 (Ala198 C=OHN of ligand) and Phe97 along with other hydrophobic interactions with Phe149, Ala157, Tyr158, Met161, Met199, Ala201, Ile202 and Leu207 of Enoyl ACP reductase. These interactions have been observed for the co-crystallized ligand of PDB 4cod. Hence this protein-ligand complex has been selected for further studies. **Figures 2a** and **3a** shows the fit of **4a** and **4d** into the active site of the receptor. The 2D plot of protein-ligand interaction diagram for the same was figured out in **2b** and **3b** respectively.

MD Simulation studies

The stability of protein-ligand complex formed by molecular modeling was then validated by implementing a MD simulation using DESMOND. The production run for the complex was carried out for 20 ns. The Simulation Quality Analysis was performed and an analysis of the total energy, potential energy, temperature, pressure, and volume over the length of the simulation was done. The analysis includes the average value, the standard deviation, and the slope of a linear fit to the values of the property as a function of time. All the values indicated a stable MD simulation production run (**Fig. 4**).

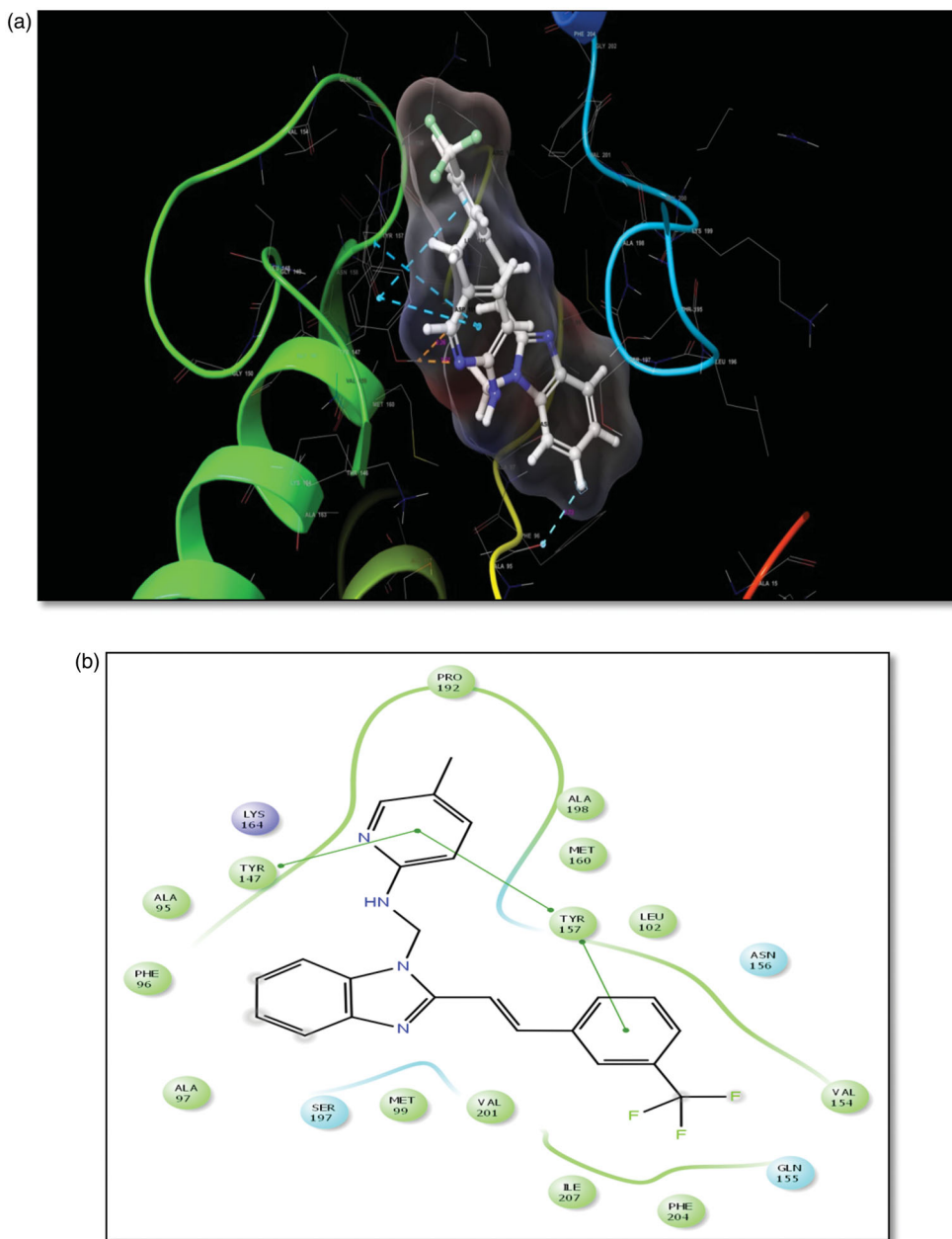


Figure 1. (a) 3D presentation of ligand **4d** interaction into the active site of long enoyl-acyl-carrier-protein reductase of *S. aureus* (4NZ9). (b) 2D presentation of ligand **4d** interacting with amino acid residues.

To explore the dynamic stability of the complex and to ensure the rationality of the sampling method, RMSD from the structure in frame 0 was analyzed on a structure in 1001 frames. The plots (Figs. 5–7) showed no significant increase in deviation until the completion of 20 ns. The ligand RMSD value was also monitored and was found to be

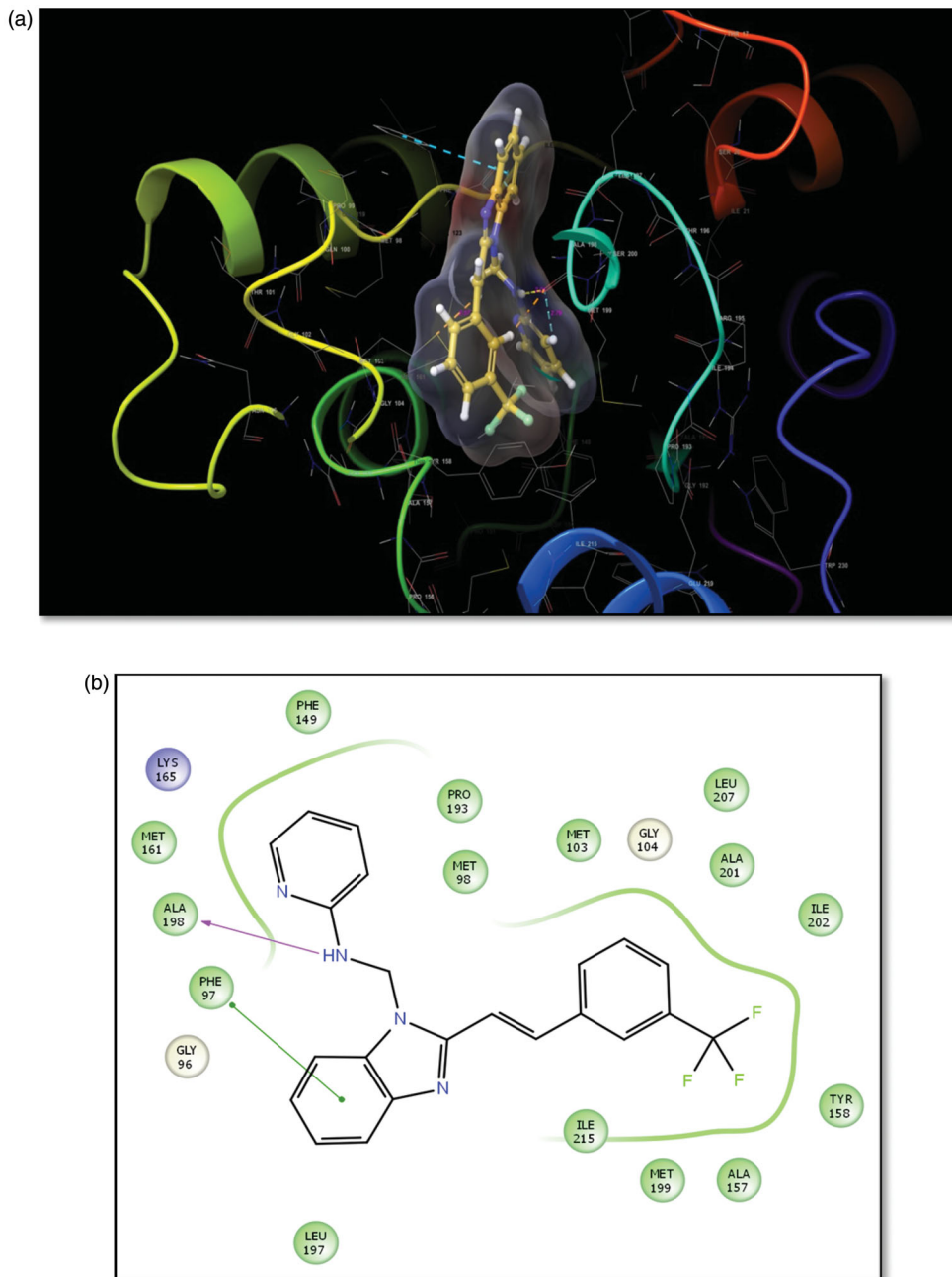


Figure 2. (a) 3D presentation of protein-ligand interactions of **4a** into the active site of an enoyl-[acyl-carrier-protein] reductase of *M. tuberculosis* (4COD). (b) 2D presentation of ligand **4a** interacting with amino acid residues.

stabilized during the production run. All the findings strongly support the high stability of the complex formed.

The descriptive analyses of RMSD of the compounds in 20 ns MD simulation from the zero frames have been given in [Table 4](#). The maximum RMSD fitted to the target

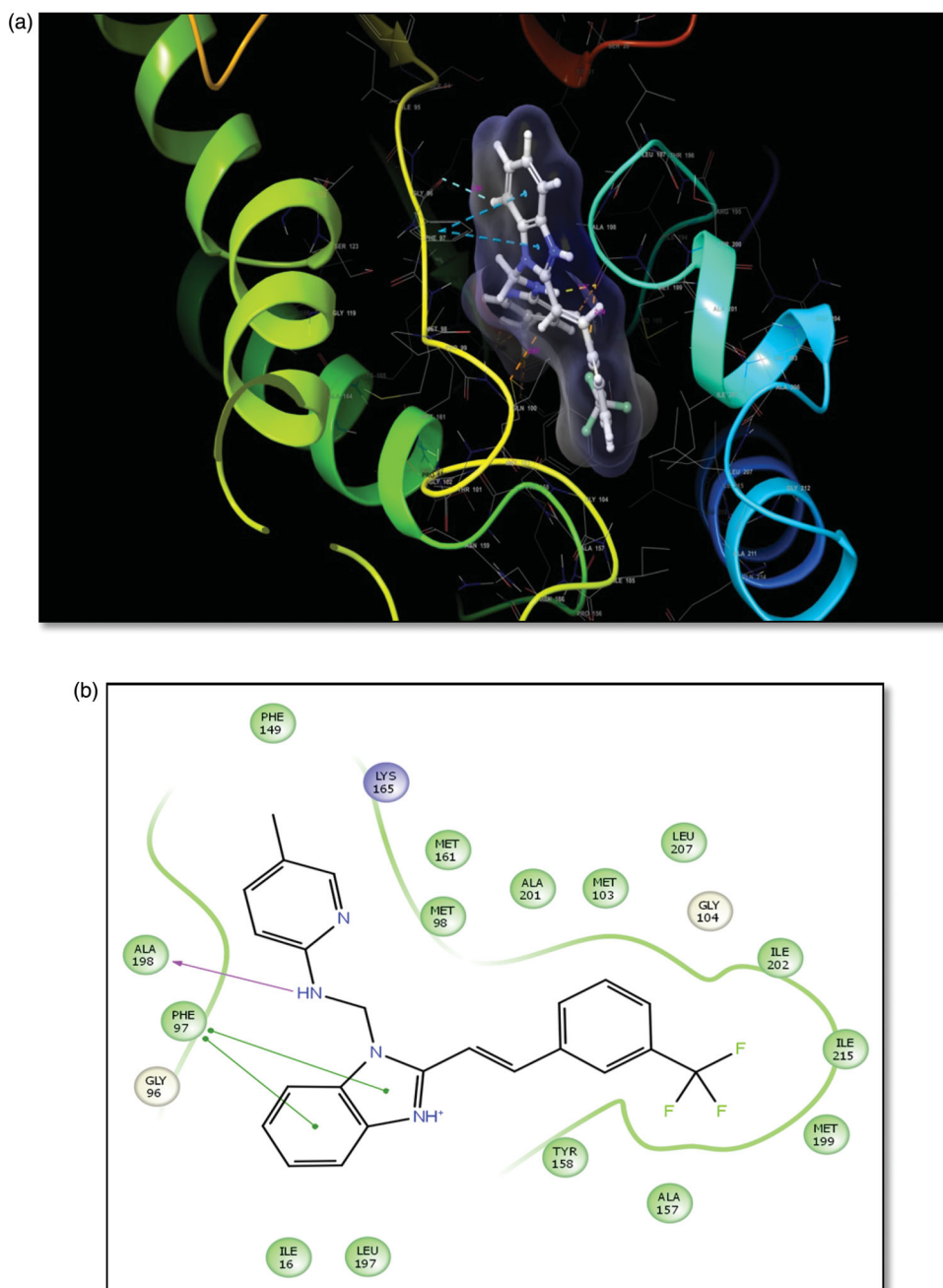


Figure 3. (a) 3D presentation of protein-ligand interactions of **4d** into the active site of an enoyl-[acyl-carrier-protein] reductase of *M. tuberculosis* (4COD). (b) 2D presentation of ligand **4d** interacting with amino acid residues.

ligand in the active pocket of Enoyl ACP reductase complex is 1.376 \AA and the standard deviation for ligand **4a** complex with Enoyl ACP reductase is 0.287 . Similarly, the mean RMSD value for C-alpha of protein was 2.104 \AA and the standard deviation being 0.252 which showed the stability ligand and protein. The plot indicates the RMSF values for

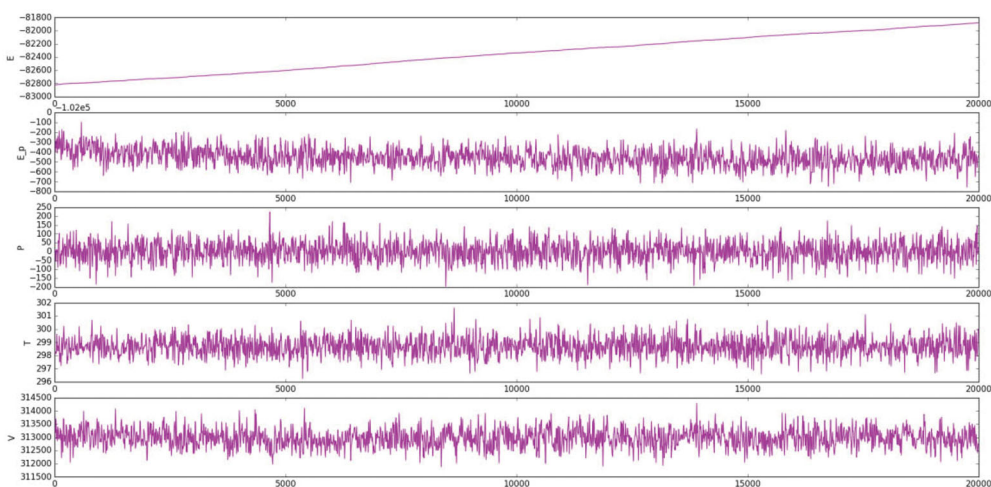


Figure 4. Simulation Quality Analysis.

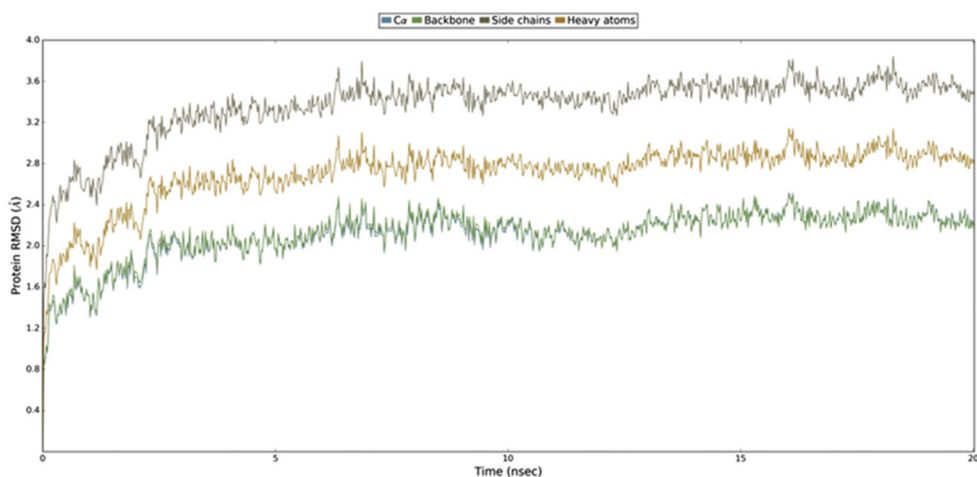


Figure 5. Protein RMSD for Backbone, Side chain and Heavy atoms.

the C-alpha atom of the residues (Fig. 8). The beginning and the end values are high as they indicate the N-terminal and C-terminal residues. The other residues have reliable RMSF values below 2 Å.

The interaction of ligand **4a** with protein was monitored throughout the simulation (Figs. 9 and 10). The stability of the hydrogen bonding network predicted by Glide XP docking method was examined by monitoring the percentage occurrence of predicted hydrogen bonds during the simulation time. The presence of some prominent hydrogen bonds between the inhibitor and Enoyl ACP protein reductase with modest to high frequencies has been observed during the analyses of the MD trajectories of input inhibitors. The molecular docking for ligand **4a** predicted one hydrogen bond for **4a**/Enoyl ACP reductase complex by GlideXP. However, this hydrogen bond (Ala198 C=O—HN of ligand), was observed only during 10% of the MD trajectory. For 52% of the simulation time, a new hydrogen bond was observed with Gln 100 (Gln100 O=C—NH—N of

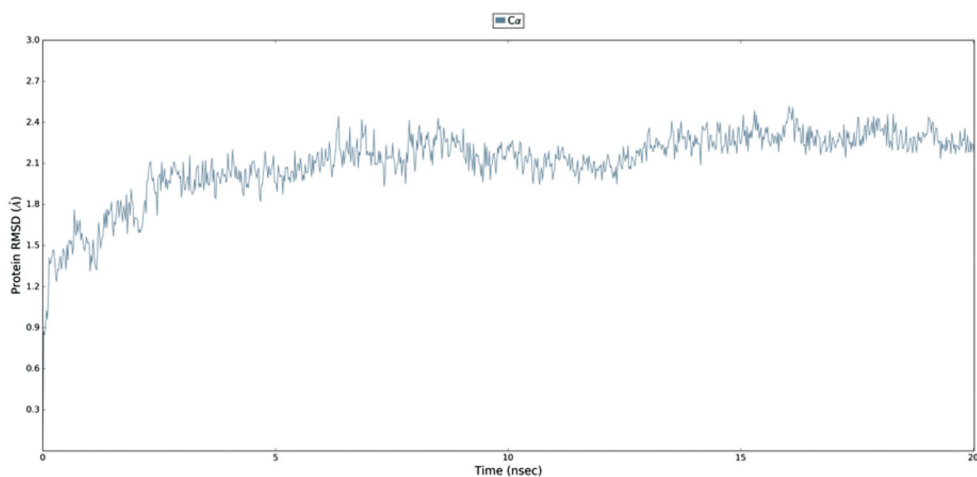


Figure 6. Protein RMSD for $C\alpha$ atoms.

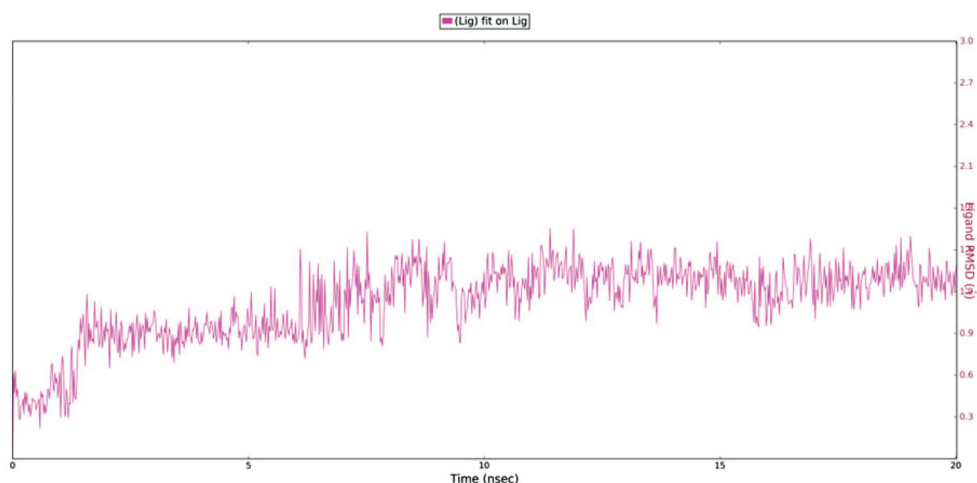


Figure 7. Ligand RMSD.

Table 4. RMSD values to compare the docked conformation.

	Mean (Å)	Median (Å)	Standard Deviation	Range (Å)
RMSD_C-alpha	2.104	2.158	0.252	0.000, 2.517
RMSD_Backbone	2.138	2.193	0.247	0.000, 2.540
RMSD_All residues	2.935	3.014	0.290	0.000, 3.366
RMSD_ligand	1.376	1.439	0.287	0.000, 1.939

ligand) as shown in the simulation interaction diagram (Fig. 11). Several strong hydrophobic interactions with Met103 have also been observed during the course of the simulation. Some hydrophobic interactions were also observed with Phe97, Phe149, Ala157, Tyr158, Met161, Met199, Ala201, Ile202 and Leu207, which were short-lived. Additionally, water bridges have been observed with Met 98, Gln 100 and Ala198 of for short period during the production run. Figure 10 represents a timeline of the interactions and contacts in terms of H-bonds, hydrophobic interactions, ionic interactions

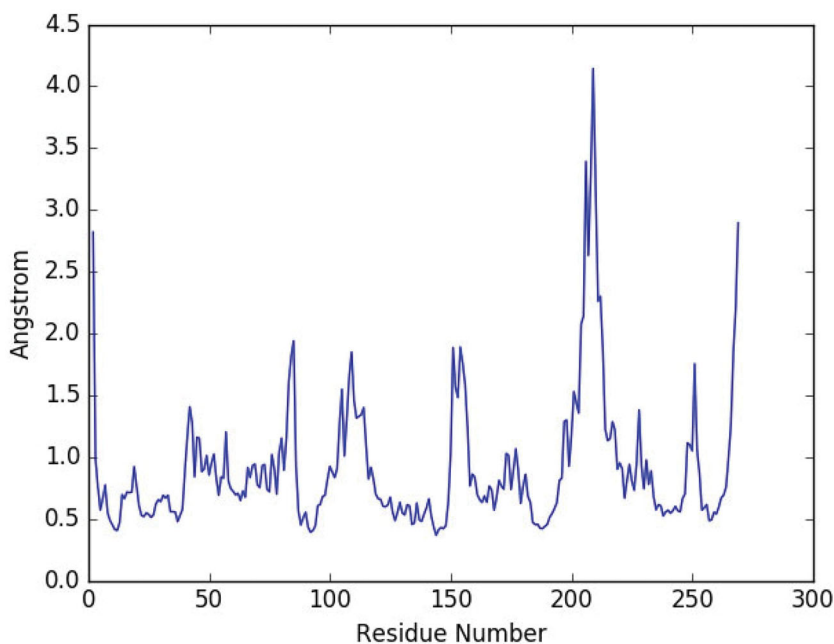


Figure 8. RMSF values for the C-alpha atom of the residues.

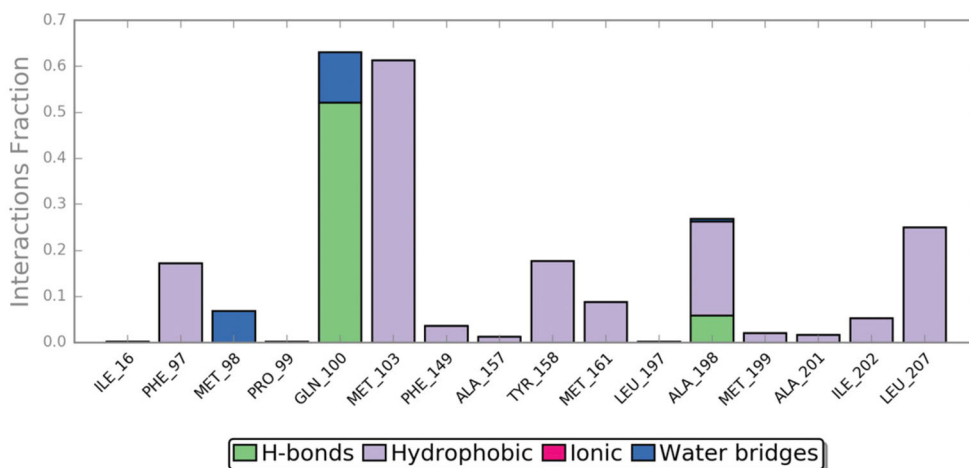


Figure 9. Histogram plot for protein-ligand contacts.

and water bridges. The top panel shows the total number of specific contacts the protein makes with the ligand over the course of the trajectory. The bottom panel shows which residues interact with the ligand in each trajectory frame. Some residues make more than one specific contact with the ligand, which is represented by a darker shade of orange, according to the scale to the right of the plot.

In silico ADMET studies. We have calculated *In silico* physicochemical properties and logarithm of partition coefficient to determine lipophilicity (Log Po/w) to forecasting Lipinski's, Ghose, Veber and Egan drug-likeness (Table 5) of final compounds using

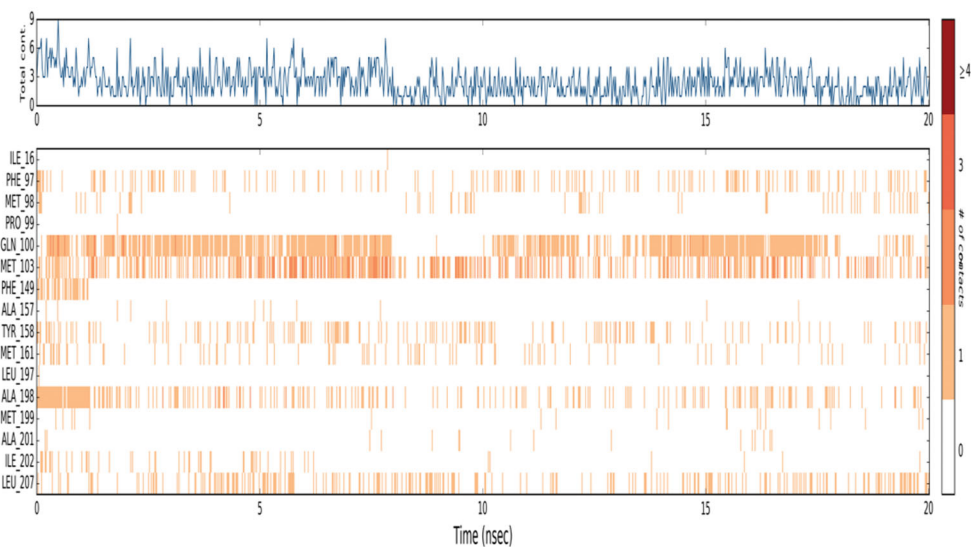


Figure 10. A timeline representation of the interactions and contacts (H-bonds, Hydrophobic, Ionic, Water bridges).

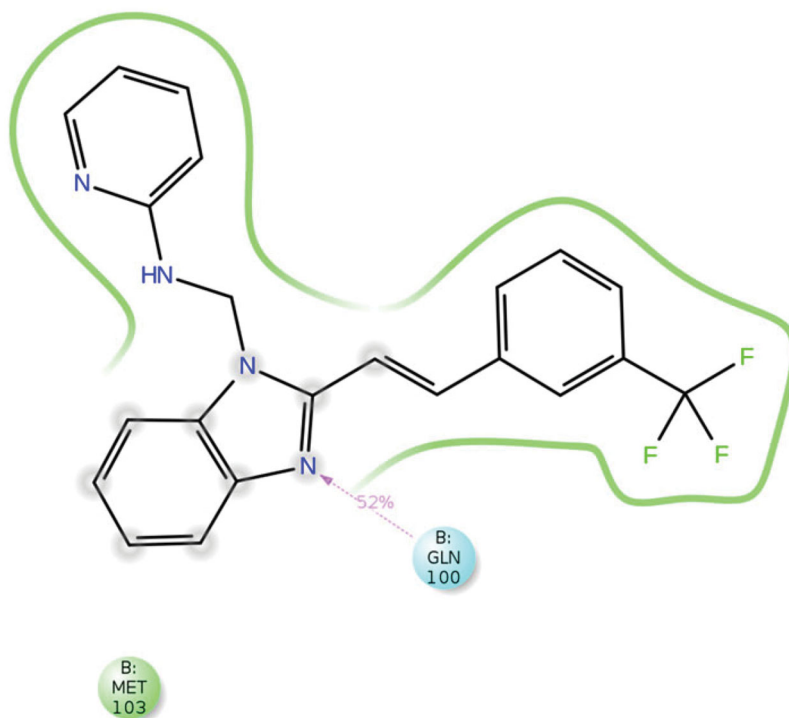


Figure 11. A schematic diagram of detailed ligand atom interactions with the protein residue at the end of simulation.

Table 5. *In silico* physicochemical properties, lipophilicity and drug likeness of **3a–e** and **4a–e** by SwissADME.

Comp. No.	Physicochemical Properties										Drug Likeness				
	MW	nHA	nAHA	nRB	nHBA	nHBD	MR	TPSA	Lipophilicity Consensus Log P	Lipinski	Ghose	Veber	Egan		
3a	301.35	23	21	4	3	1	90.85	55.63	2.6	Yes	Yes	Yes	Yes		
3b	301.35	23	21	4	3	1	90.85	55.63	2.49	Yes	Yes	Yes	Yes		
3c	301.35	23	21	4	3	1	90.85	55.63	2.47	Yes	Yes	Yes	Yes		
3d	315.37	24	21	4	3	1	95.81	55.63	2.95	Yes	Yes	Yes	Yes		
3e	393.44	30	27	6	4	1	117.36	64.86	3.71	Yes	Yes	Yes	Yes		
4a	394.39	29	21	6	5	1	107.99	42.74	4.75	Yes	No; 1 violation	Yes	No; 1 violation		
4b	394.39	29	21	6	5	1	107.99	42.74	4.7	Yes	No; 1 violation	Yes	No; 1 violation		
4c	394.39	29	21	6	5	1	107.99	42.74	4.67	Yes	No; 1 violation	Yes	No; 1 violation		
4d	408.42	30	21	6	5	1	112.95	42.74	5.13	Yes	No; 1 violation	Yes	No; 1 violation		
4e	486.49	36	27	8	6	1	134.5	51.97	5.93	No; 1 violation	No; 3 violations	Yes	No; 1 violation		

Table 6. *In silico* pharmacokinetics of 3a-e and 4a-e by SwissADME.

Comp. No	GI absorption	BBB permeant	Pgp substrate	CYP1A2 inhibitor	CYP2C19 inhibitor	CYP2C9 inhibitor	CYP2D6 inhibitor	CYP3A4 inhibitor	log Kp (cm/s)
3a	High	Yes	Yes	Yes	Yes	Yes	Yes	Yes	-6.00
3b	High	Yes	Yes	Yes	Yes	Yes	Yes	Yes	-6.24
3c	High	Yes	Yes	Yes	Yes	Yes	Yes	Yes	-6.24
3d	High	Yes	Yes	Yes	Yes	Yes	Yes	Yes	-5.83
3e	High	Yes	Yes	Yes	Yes	Yes	Yes	Yes	-5.48
4a	High	No	No	Yes	Yes	Yes	Yes	Yes	-4.73
4b	High	No	No	Yes	Yes	Yes	Yes	Yes	-4.96
4c	High	No	No	Yes	Yes	Yes	Yes	Yes	-4.96
4d	High	No	No	Yes	Yes	Yes	Yes	No	-4.55
4e	Low	No	No	No	Yes	No	Yes	No	-4.21

SwissADME. Screening of *Lipinski's Rule of Five* and Veber filters showed that all the synthesized compounds meet the criteria of drug-likeness assessment, however in Ghose and Egan filter screening showed that compounds **3a-e** meets all the criteria whereas **4a**, **4b**, **4c** and **4d** rejected with one violation. Pharmacokinetics for the same was evaluated by using SwissADME online web tool and results have been incorporated in [Table 6](#). All the compounds showed high gastrointestinal absorption except **4e**. Mannich derivative **3a-e** exhibited BBB permeability, whereas **4a-e** found to have no permeability. A similar trend has been observed for p-glycoprotein substrate. Cytochrome P450 (CYP) isoforms are responsible for metabolism of many drugs. Inhibition of CYP isoforms results in decreased elimination and change in metabolic pathways of their substrates, which is the major cause of adverse drug-drug interactions. It is, therefore, essential to trace out the potential of the compounds for CYP inhibition. The inhibitory ability (CYP3A4, CYP2D6, CYP2C19, CYP2C9 and CYP1A2) of the synthesized compounds were summarized in [Table 6](#). Most of all the newer Mannich derivatives found the inhibitor of cytochrome P450 isoforms (CYP2C19 and CYP2D6). Except for **4d**, all the derivatives found the inhibitors of other cytochrome P450 isoforms (CYP1A2 and CYP2C9). **4d** and **4e** showed no ability to inhibit CYP3A4. The values of Log Kp indicate the skin permeation for the respective inputs. The computational toxicity predictions can help to reduce the number of animal experiments and save animal lives. From the wet lab and molecular modeling results, four compounds viz., **3d**, **4a**, **4b** and **4d** have been selected for further screening to analyze their overall drug score and toxicity risks. *In silico* toxicology predictions were evaluated by using ProTox-II and results are given in [Table 7](#). All the selected compounds had LD₅₀ values between 500–1360 mg/kgBodyWeight and belong to class IV Global Harmoni System (GHS) indicating that it could be harmful if swallowed. As all the compounds belong to class IV, it is predicted to found moderate to mild toxicity. Higher the value of LD₅₀ displayed the lower its toxicity. **4a** was of moderate toxicity with the LD₅₀ value of 1360 mg/kgBW. From the results, it is predicted that all the selected compounds have no hepatotoxicity and cytotoxicity. As the inputs showed inactive to organ toxicity, it can be predicted that these inputs have no toxic effect on the liver. Moreover results predicted to have mutagenic toxicity for all four inputs and active immunotoxicity expect **3d**.

Table 7. *In silico* toxicology prediction of **3d**, **4a**, **4b** and **4d** by ProTox.

Comp. No	Oral toxicity prediction*		Organ toxicity (Probability)	Toxicity end point (Probability)			
	Predicted LD ₅₀ mg/kg	Predicted toxicity class		Hepatotoxicity	Carcinogenicity	Immunotoxicity	Mutagenicity
3d	500	4	Inactive (0.71)	Active (0.59)	Inactive (0.9)	Active (0.65)	Inactive (0.78)
4a	1360	4	Inactive (0.59)	Active (0.58)	Active (0.96)	Active (0.59)	Inactive (0.81)
4b	1000	4	Inactive (0.59)	Active (0.58)	Active (0.96)	Active (0.59)	Inactive (0.81)
4d	1000	4	Inactive (0.58)	Active (0.58)	Active (0.96)	Active (0.59)	Inactive (0.80)

*Prediction accuracy 54.26 % for **3d**, **4a**, **4b** and **4d**.

Experimental

Reduce pressure distillation has been employed to remove and recover the solvents. Melting points were determined by the open tube capillary method and are uncorrected. The reaction was monitored by TLC plates (silica gel G) using different eluent system and visualized under ultraviolet (UV) light, or iodine vapor. The IR spectra were obtained on Thermo scientific Nicolet iS10 & Agilent Resolution Pro FT-IR spectrometer (KBr pellets). The ¹H-NMR spectra were recorded on a Bruker Avance II 400 MHz while ¹³C NMR spectra 100 MHz spectrometers using Trimethylsilane (TMS) as the internal standard in deuterated dimethylsulfoxide (DMSO-*d*₆) & deuterated chloroform (CDCl₃) solvents. Chemical shifts were reported in ppm units with the use of δ scale. The mass spectra were recorded by Waters, Q-TOF micromass (ESI-MS), SAIF, Chandigarh. The microwave induced synthesis were carried out in a “QPro-M Modified Microwave Synthesis System” manufactured by Questron Technologies Corporation, Ontario L4Z 2E9 Canada, whereby microwaves are generated by magnetron at a frequency of 2450 MHz having an output energy range of 100–500 W. The QPro-M designed as multimode microwave cavity to perform faster Digestion (Open vessel), evaporation, extraction and synthesis with ease.

3-Trifluoromethyl-cinnamic acid required to synthesize the key intermediate (**2**) has been synthesized as described in the literature.^[35] Other than this, all the reagents or starting materials used for the synthesis were taken directly and were used without further purification and the solvents used were LR and AR grade. Full experimental detail of the synthesis and characterization of intermediate (**1**) and (**2**) has been given in the supporting information.

General procedure for synthesis of (**3a–e**) & (**4a–e**)

Benzo[*d*]imidazole (**1**) or (**2**) (1.0 mmol) was dissolved in methanol (10 vol). To this solution, 0.19 mL 37% formaldehyde was added and stirred at 5–10 °C for about 10 min. Then a solution of substituted amino pyridine (1.0 equiv) in methanol (10 vol) was added drop wise to resulting reaction mixture at the same temperature with vigorous stirring for 1 h. The reaction mixture was then introduced to the microwave oven and was irradiated for 8–9 min at 60–65 °C (300 W) while monitoring the course of reaction by TLC (using dichloromethane: methanol, 9:11). Then after reaction mass was kept overnight at room temperature. The resulting solid was collected by filtration, washed with cold petroleum ether (2 X 2.5 mL), dried and recrystallized from ethanol to obtained pure (**3a–e**) & (**4a–e**). *N*-((2-(pyridin-4-yl)-1H-benzo[*d*]imidazol-1-

yl)methyl)pyridin-2-amine (3a) Yield 87%, m.p. 218–220 °C, IR (KBr) ν cm^{-1} : 3396 (N-H), 3055, 2936 (aromatic C-H), 2868 (methylene C-H, str.), 1606 (C=N), 1430 (methylene C-H, bend.), 1350 (C-N); ^1H NMR (400 MHz, DMSO- d_6) δ (ppm): 8.59 (t, 1H, NH, disappeared on D_2O exchange), 8.32–7.71 (m, 4H, CH, aromatic; 4-pyridine), 7.46–7.08 (m, 8H, CH, aromatic; 2-pyridine & benzimidazole), 5.02 (d, 2H, CH_2); ^{13}C NMR (100 MHz, DMSO- d_6) δ (ppm): (150.47; N-C=N), (149.78, 135.19, 121.43; 4-pyridine), (145.66, 140.75, 137.09, 123.67, 119.02; 2-pyridine), (122.58, 120.30, 118.53, 111.13, 106.79, 105.48; benzimidazole), 61.41 (CH_2); ESI-MS: m/z calculated 301.13, found $[\text{M} + \text{H}]^+$ 302.13; Anal. Calcd. for $\text{C}_{18}\text{H}_{15}\text{N}_5$: C, 71.74; H, 5.02; N, 23.24. Found: C, 71.65; H, 4.93; N, 23.13%.

Full experimental protocol to synthesize (**3b–e**) and (**4a–e**) with their characterization data has been proved in the [supporting information](#).

Conclusion

The present article deals with the synthesis of newer analogous of benz[*d*]imidazoles which were synthesized by *N*-Mannich reaction using different pyridine amines by MW induced synthetic approach. The synthetic pathways explain the edge of MW assisted synthesis with the simplicity of procedure, increased reaction rate and escalate product yields. These derivatives assessed for their antimicrobial, antituberculosis and antiprotozoal activity. Modification in key intermediate **1** and **2**, impact the potency against different biological target. The electron releasing group on pyridine ring attached 2-(pyridin-4-yl)-1*H*-benzo[*d*]imidazole showed potency against *T. cruzi*. The antimicrobial and antifungal potency of **4d** explains the key factor responsible for its potency is the presence of electron realizing group on pyridine component along with the styryl functionality in benz[*d*]imidazole. Hence, the modification of amine component with various electron releasing and electron withdrawing substituents impact the biological profile of derived motif against different biological target. **4d** showed very good binding energy in the active pocket of enoyl ACP reductase of *S. aureus* with -11.792 docking score. It was also observed that the promising antimicrobials have proved to be encouraging antitubercular. The change in the position of nitrogen atom in pyridine ring attached 2-(3-(trifluoromethyl)styryl)-1*H*-benzo[*d*]imidazole plays an important role to attain better antimycobacterial activity as well as *in-vitro* leishmanicidal effect. Compound **4a** showed potency against *M. tuberculosis* H37Rv strain along with Glide XP Gscore -11.266 . Based on GlideXP docking simulations, one hydrogen bond with Ala198 and one pi-pi inaction with Phe97 were predicted for the compound **4a** to Enoyl ACP reductase complex. However, this hydrogen bond was observed during 10% of the MD trajectory and for 52% of the simulation time, a new interaction was observed with Gln 100 (Gln100 O=C–NH–N of ligand) displaying the stability of the protein-ligand complex. *In silico* predicated toxicity results and calculated physicochemical properties, lipophilicity, pharmacokinetic parameters give the best choice for the preparation of new derivatives with improved antitubercular and antiprotozoal activity in the future.

Acknowledgments

The authors are thankful to Veer Narmad South Gujarat University for providing necessary facilities. The authors are thankful to Dr. Dhanji Rajani, Microcare Laboratory, Surat, for antimicrobial activity.

Disclosure statement

The authors declared no conflict of interest.

ORCID

Vatsal M. Patel  <http://orcid.org/0000-0002-2286-1915>

References

- [1] Enciso, E.; Sarmiento-Sánchez, J. I.; López-Moreno, H. S.; Ochoa-Terán, A.; Osuna-Martínez, U.; Beltrán-López, E. Synthesis of New Quinazolin-2, 4-Diones as anti-Leishmania mexicana Agents. *Mol. Divers.* **2016**, *20*, 821–828. DOI: [10.1007/s11030-016-9693-8](https://doi.org/10.1007/s11030-016-9693-8).
- [2] Patel, N. B.; Patel, J. N.; Purohit, A. C.; Patel, V. M.; Rajani, D. P.; Moo-Puc, R.; Lopez-Cedillo, J. C.; Nogueada-Torres, B.; Rivera, G. In Vitro and in Vivo Assessment of Newer Quinoxaline–Oxadiazole Hybrids as Antimicrobial and Antiprotozoal Agents. *Int. J. Antimicrob. Agents.* **2017**, *50*, 413–418. DOI: [10.1016/j.ijantimicag.2017.04.016](https://doi.org/10.1016/j.ijantimicag.2017.04.016).
- [3] World Health Organization. Global tuberculosis report 2019. In *Global tuberculosis report 2019*, 2019.
- [4] Ahirrao, P. Recent Developments in Antitubercular Drugs. *MRRMC.* **2008**, *8*, 1441–1451. DOI: [10.2174/138955708786786516](https://doi.org/10.2174/138955708786786516).
- [5] Luckner, S. R.; Liu, N.; Am Ende, C. W.; Tonge, P. J.; Kisker, C. A Slow, Tight Binding Inhibitor of InhA, the Enoyl-Acyl Carrier Protein Reductase from *Mycobacterium tuberculosis*. *J. Biol. Chem.* **2010**, *285*, 14330–14337. DOI: [10.1074/jbc.M109.090373](https://doi.org/10.1074/jbc.M109.090373).
- [6] Patel, V. M.; Patel, N. B.; Chan-Bacab, M. J.; Rivera, G. Synthesis, Biological Evaluation and Molecular Dynamics Studies of 1, 2, 4-Triazole Clubbed Mannich Bases. *Comput. Biol. Chem.* **2018**, *76*, 264–274. DOI: [10.1016/j.compbiolchem.2018.07.020](https://doi.org/10.1016/j.compbiolchem.2018.07.020).
- [7] Khan, I.; Patel, N. B.; Patel, V. M. Synthesis, in Silico Molecular Docking and Pharmacokinetic Studies, in Vitro Antimycobacterial and Antimicrobial Studies of New Imidazolones Clubbed with Thiazolidinedione. *CAD.* **2018**, *14*, 269–283. DOI: [10.2174/15734099146666180516113552](https://doi.org/10.2174/15734099146666180516113552).
- [8] Spasov, A.; Yozhitsa, I.; Bugaeva, L.; Anisimova, V. Benzimidazole Derivatives: Spectrum of Pharmacological Activity and Toxicological Properties (a Review). *Pharm. Chem. J.* **1999**, *33*, 232–243. DOI: [10.1007/BF02510042](https://doi.org/10.1007/BF02510042).
- [9] Saha, P.; Ramana, T.; Purkait, N.; Ali, M. A.; Paul, R.; Punniyamurthy, T. Ligand-Free Copper-Catalyzed Synthesis of Substituted Benzimidazoles, 2-Aminobenzimidazoles, 2-Aminobenzothiazoles, and Benzoxazoles. *J. Org. Chem.* **2009**, *74*, 8719–8725. DOI: [10.1021/jo901813g](https://doi.org/10.1021/jo901813g).
- [10] Wang, H.; Wang, Y.; Peng, C.; Zhang, J.; Zhu, Q. A Direct Intramolecular C–H Amination Reaction Cocatalyzed by Copper (II) and Iron (III) as Part of an Efficient Route for the Synthesis of Pyrido [1, 2-a] Benzimidazoles from N-Aryl-2-Aminopyridines. *J. Am. Chem. Soc.* **2010**, *132*, 13217–13219. DOI: [10.1021/ja1067993](https://doi.org/10.1021/ja1067993).
- [11] Saify, Z. S.; Kamil, A.; Akhtar, S.; Taha, M.; Khan, A.; Khan, K. M.; Jahan, S.; Rahim, F.; Perveen, S.; Choudhary, M. I. 2-(2'-Pyridyl) Benzimidazole Derivatives and Their Urease Inhibitory Activity. *Med. Chem. Res.* **2014**, *23*, 4447–4454. DOI: [10.1007/s00044-014-1015-z](https://doi.org/10.1007/s00044-014-1015-z).

- [12] Lu, J.; Yang, B.; Bai, Y. Microwave Irradiation Synthesis of 2-Substituted Benzimidazoles Using PPA as a Catalyst under Solvent-Free Conditions. *Synth. Commun.* **2002**, *32*, 3703–3709. DOI: [10.1081/SCC-120015381](https://doi.org/10.1081/SCC-120015381).
- [13] VanVliet, D. S.; Gillespie, P.; Sciacinski, J. J. Rapid One-Pot Preparation of 2-Substituted Benzimidazoles from 2-Nitroanilines Using Microwave Conditions. *Tetrahedron Lett.* **2005**, *46*, 6741–6743. DOI: [10.1016/j.tetlet.2005.07.130](https://doi.org/10.1016/j.tetlet.2005.07.130).
- [14] Demirayak, S.; Kayagil, I.; Yurttas, L. Microwave Supported Synthesis of Some Novel 1, 3-Diarylpyrazino [1, 2-a] Benzimidazole Derivatives and Investigation of Their Anticancer Activities. *Eur. J. Med. Chem.* **2011**, *46*, 411–416. DOI: [10.1016/j.ejmech.2010.11.007](https://doi.org/10.1016/j.ejmech.2010.11.007).
- [15] Mentese, E.; Bektaş, H.; Ülker, S.; Bekircan, O.; Kahveci, B. Microwave-Assisted Synthesis of New Benzimidazole Derivatives with Lipase Inhibition Activity. *J. Enzyme Inhib. Med. Chem.* **2014**, *29*, 64–68. DOI: [10.3109/14756366.2012.753880](https://doi.org/10.3109/14756366.2012.753880).
- [16] Shah, K.; Chhabra, S.; Shrivastava, S. K.; Mishra, P. Benzimidazole: A Promising Pharmacophore. *Med. Chem. Res.* **2013**, *22*, 5077–5104. DOI: [10.1007/s00044-013-0476-9](https://doi.org/10.1007/s00044-013-0476-9).
- [17] Noolvi, M.; Agrawal, S.; Patel, H.; Badiger, A.; Gaba, M.; Zambre, A. Synthesis, Antimicrobial and Cytotoxic Activity of Novel Azetidine-2-One Derivatives of 1H-Benzimidazole. *Arab. J. Chem.* **2014**, *7*, 219–226. DOI: [10.1016/j.arabjch.2011.02.011](https://doi.org/10.1016/j.arabjch.2011.02.011).
- [18] Tonelli, M.; Simone, M.; Tasso, B.; Novelli, F.; Boido, V.; Sparatore, F.; Paglietti, G.; Prich, S.; Giliberti, G.; Blois, S. Antiviral Activity of Benzimidazole Derivatives. II. Antiviral Activity of 2-Phenylbenzimidazole Derivatives. *Bioorg. Med. Chem.* **2010**, *18*, 2937–2953. DOI: [10.1016/j.bmc.2010.02.037](https://doi.org/10.1016/j.bmc.2010.02.037).
- [19] Navarrete-Vázquez, G.; Cedillo, R.; Hernández-Campos, A.; Yépez, L.; Hernández-Luis, F.; Valdez, J.; Morales, R.; Cortés, R.; Hernández, M.; Castillo, R. Synthesis and Antiparasitic Activity of 2-(Trifluoromethyl) Benzimidazole Derivatives. *Bioorg. Med. Chem. Lett.* **2001**, *11*, 187–190. DOI: [10.1016/S0960-894X\(00\)00619-3](https://doi.org/10.1016/S0960-894X(00)00619-3).
- [20] El, A. R.; Aboul-Enein, H. Y. Benzimidazole Derivatives as Potential Anticancer Agents. *Mini Rev. Med. Chem.* **2013**, *13*, 399–407.
- [21] Iwahi, T.; Satoh, H.; Nakao, M.; Iwasaki, T.; Yamazaki, T.; Kubo, K.; Tamura, T.; Imada, A. Lansoprazole, a Novel Benzimidazole Proton Pump Inhibitor, and Its Related Compounds Have Selective Activity against *Helicobacter pylori*. *Antimicrob. Agents Chemother.* **1991**, *35*, 490–496. DOI: [10.1128/AAC.35.3.490](https://doi.org/10.1128/AAC.35.3.490).
- [22] Abdel-Aziz, H. A.; Gamal-Eldeen, A. M.; Hamdy, N. A.; Fakhr, I. M. Immunomodulatory and Anticancer Activities of Some Novel 2-Substituted-6-Bromo-3-Methylthiazolo [3, 2-a] Benzimidazole Derivatives. *Arch. Pharm. Chem. Life. Sci.* **2009**, *342*, 230–237. DOI: [10.1002/ardp.200800189](https://doi.org/10.1002/ardp.200800189).
- [23] Sircar, J. C.; Richards, M. L. Benzimidazole compounds for modulating IgE and inhibiting cellular proliferation. Google Patents: 2007.
- [24] Selvakumar, S.; Babu, I. S.; Chidambaranathan, N. In-Vivo Central Nervous System- Locomotor Activity of Some Synthesized 2-[(1-((Phenyl Amino) Methyl) Substituted 1-Benzimidazol-2-yl) Alkyl] Isoindoline-1, 3-Diones. *Biosci, Biotechnol. Res. Asia* **2013**, *10*, 937–943. DOI: [10.13005/bbra/1222](https://doi.org/10.13005/bbra/1222).
- [25] El-Masry, A.; Fahmy, H.; Ali Abdelwahed, S. Synthesis and Antimicrobial Activity of Some New Benzimidazole Derivatives. *Molecules* **2000**, *5*, 1429–1438. DOI: [10.3390/51201429](https://doi.org/10.3390/51201429).
- [26] Xu, Z.; Zhang, S.; Gao, C.; Fan, J.; Zhao, F.; Lv, Z.-S.; Feng, L.-S. Isatin Hybrids and Their anti-Tuberculosis Activity. *Chin. Chem. Lett.* **2017**, *28*, 159–167. DOI: [10.1016/j.ccllet.2016.07.032](https://doi.org/10.1016/j.ccllet.2016.07.032).
- [27] Taher, A. T.; Khalil, N. A.; Ahmed, E. M. Synthesis of Novel Isatin-Thiazoline and Isatin-Benzimidazole Conjugates as anti-Breast Cancer Agents. *Arch. Pharm. Res.* **2011**, *34*, 1615–1621. DOI: [10.1007/s12272-011-1005-3](https://doi.org/10.1007/s12272-011-1005-3).
- [28] Shingare, M.; Mane, D.; Shinde, D.; Thore, S.; Bhawsar, S. Synthesis of Mannich Bases of Benzimidazole as Possible Antiviral Agents. *Asian J. Chem.* **1996**, *8*, 225.
- [29] Jesudason, E. P.; Sridhar, S.; Malar, E. P.; Shanmugapandiyar, P.; Inayathullah, M.; Arul, V.; Selvaraj, D.; Jayakumar, R. Synthesis, Pharmacological Screening, Quantum Chemical

- and in Vitro Permeability Studies of N-Mannich Bases of Benzimidazoles through Bovine Cornea. *Eur. J. Med. Chem.* **2009**, *44*, 2307–2312. DOI: [10.1016/j.ejmech.2008.03.043](https://doi.org/10.1016/j.ejmech.2008.03.043).
- [30] Kumar, S. V.; Subramanian, M. R.; Chinnaiyan, S. K. Synthesis, Characterisation and Evaluation of N-Mannich Bases of 2-Substituted Benzimidazole Derivatives. *J. Young Pharm.* **2013**, *5*, 154–159. DOI: [10.1016/j.jyp.2013.11.004](https://doi.org/10.1016/j.jyp.2013.11.004).
- [31] A Datar, P.; A Limaye, S. Design and Synthesis of Mannich Bases as Benzimidazole Derivatives as Analgesic Agents. *AIAAMC.* **2015**, *14*, 35–46. DOI: [10.2174/1871523014666150312164625](https://doi.org/10.2174/1871523014666150312164625).
- [32] He, X.; Alian, A.; Stroud, R.; Ortiz de Montellano, P. R. Pyrrolidine Carboxamides as a Novel Class of Inhibitors of Enoyl Acyl Carrier Protein Reductase from *Mycobacterium tuberculosis*. *J. Med. Chem.* **2006**, *49*, 6308–6323. DOI: [10.1021/jm060715y](https://doi.org/10.1021/jm060715y).
- [33] Aparna, Y.; Sharada, L.; Subhashini, N.; Sreekanth, S. Synthesis, Characterization, Molecular Docking, and Antimicrobial Activity of New Arylidene-Substituted Imidazoles. *Russ. J. Gen. Chem.* **2019**, *89*, 1202–1208. DOI: [10.1134/S1070363219060161](https://doi.org/10.1134/S1070363219060161).
- [34] Lima, C. H. d S.; de Alencastro, R. B.; Kaiser, C. R.; de Souza, M. V. N.; Rodrigues, C. R.; Albuquerque, M. G. Aqueous Molecular Dynamics Simulations of the M. tuberculosis enoyl-ACP reductase-NADH System and Its Complex with a Substrate Mimic or Diphenyl Ethers Inhibitors. *IJMS.* **2015**, *16*, 23695–23722. DOI: [10.3390/ijms161023695](https://doi.org/10.3390/ijms161023695).
- [35] Bijukumar, G.; Maloyesh, B.; Bhaskar, B. S.; Rajendra, A. Efficient Synthesis of Cinacalcet Hydrochloride. *Synth. Commun.* **2008**, *38*, 1512–1517. DOI: [10.1080/00397910801928541](https://doi.org/10.1080/00397910801928541).